Src and Wnt signaling regulate dynactin accumulation to the P2-EMS cell border in *C. elegans* embryos

Haining Zhang[1,2], Ahna R. Skop[1] and John G. White[2,3,*]

[1]Laboratory of Genetics, [2]Laboratory of Molecular Biology and [3]Department of Anatomy, University of Wisconsin, Madison, WI 53706, USA
*Author for correspondence (e-mail: jwhite1@wisc.edu)

Accepted 22 October 2007
Journal of Cell Science 121, 155-161 Published by The Company of Biologists 2008
doi:10.1242/jcs.015966

Summary

In many organisms, the dynein-dynactin complex is required for the alignment of the mitotic spindle onto the axis of polarity of a cell undergoing asymmetric cell division. How this complex transduces polarity cues, either intrinsic or extrinsic, and rotationally aligns the spindle accordingly is not well understood. The *Caenorhabditis elegans* blastomere P2 polarizes the neighboring EMS blastomere, which causes the EMS spindle to rotationally align along the defined axis of polarity via two redundant signaling pathways: Wnt and Src. Here, we describe how components of the dynactin complex became locally enriched at the P2-EMS border prior to and during rotational alignment of their spindles. Wnt and Src signaling were required for both localized dynactin enrichment, and for rotational alignment of the P2 and EMS spindles. Depleting the trimeric G-protein subunit Gα did not abolish dynactin accumulation to the P2-EMS border, yet both EMS and P2 spindles failed to rotationally align, indicating that Gα might act to regulate dynein/dynactin motor activity. By RNAi of a weak *dnc-1(ts)* allele, we showed that dynactin activity was required at least for EMS spindle rotational alignment.

Supplementary material available online at
http://jcs.biologists.org/cgi/content/full/121/2/155/DC1

Key words: Src and Wnt signaling, Dynactin, Enrichment, P2-EMS border

Introduction

Asymmetric cell division is an important mechanism for generating cell diversity (Horvitz and Herskowitz, 1992; Roegiers and Jan, 2004). In general, cell polarization, mediated by intrinsic or extrinsic signals, causes the differential segregation of specific cytoplasmic components along the axis of polarity. In order to correctly partition these segregated cytoplasmic components to different daughter cells, the mitotic apparatus needs to rotationally align along the axis of polarity. In early embryogenesis in *C. elegans*, the six founder cells are produced by a series of asymmetric cell divisions (Guo and Kemphues, 1996). Among these asymmetric cell divisions, P2 and EMS blastomeres (daughters of P1), provide examples of both cell-autonomous and inductive polarization. P2 is polarized by intrinsic PAR proteins (Bowerman et al., 1997) and the mitotic spindle rotates autonomously from the dorsoventral (D-V) axis to the anteroposterior (A-P) axis (Goldstein, 2000; Hyman and White, 1987). Polarization of EMS requires cell-cell contact with P2; this contact not only specifies the endoderm fate of one of the EMS daughter cells (Goldstein, 1992; Goldstein, 1993; Goldstein, 1995a), but also properly positions the mitotic spindle of EMS along the A-P axis (Bei et al., 2002; Schlesinger et al., 1999; Thorpe et al., 1997). Two redundant pathways, Wnt and Src signaling, are required for this P2-EMS signaling. Disrupting individual pathways only leads to partial defects in EMS spindle alignment and endoderm induction (Bei et al., 2002; Schlesinger et al., 1999; Thorpe et al., 1997; Walston et al., 2004). Defective Src signaling also causes P2 spindle alignment defects, suggesting that it signals bidirectionally between P2 and EMS to control division orientation in both EMS and P1 (Bei et al., 2002). When the two pathways are impaired simultaneously, EMS no longer produces endoderm and the mitotic spindle fails completely to rotate from the left-right (L-R) to the A-P axis (Bei et al., 2002; Walston et al., 2004). In the Src pathway, both the tyrosine kinase receptor MES-1 and the downstream target phosphotyrosine accumulate to the P2-EMS border (Bei et al., 2002). One of the Wnt pathway components, DSH-2, is also localized to the P2-EMS border (Walston et al., 2004). These asymmetric enrichments of Src and Wnt signaling molecules at the P2-EMS border might be transduced to the downstream machinery to rotationally align the mitotic spindle in EMS and/or P2. Interestingly, it was found that GPR-1/2, the activator of Gα, enriches to the P2-EMS border in response to Src, but not the Wnt pathway (Tsou et al., 2003). Gα/GPR-1/2 is involved in EMS spindle rotation, possibly by upregulating the force generation from the cortex on centrosomes (Tsou et al., 2003). It remains to be determined what the role of Wnt is in regulating EMS spindle rotation, and whether the intrinsically determined P2 and the extrinsically determined EMS asymmetric divisions use the same or different motor protein(s) to rotationally align their spindles.

Dynactin is the activator of the minus-end motor dynein (Schroer, 2004). In many organisms, the dynein-dynactin complex is required for the alignment of the mitotic spindle onto the axis of polarity of a cell undergoing asymmetric cell division (Ahringer, 2003; Dujardin and Vallee, 2002; Schuyler and Pellman, 2001). However, the molecular mechanism that coordinates dynein-dynactin localization (or activity) with polarity signals, either intrinsic or extrinsic, is not well understood. In *C. elegans*, dynactin is involved in spindle alignment in both P0 and P1 (Gonczy et al., 1999a; Skop and White, 1998), the spindle rotations of which are

cell-autonomous (Goldstein, 2000). Dynactin localizes at the polar body extrusion site in the P0 cell as well as in the midbody remnant after P0 cleaves (Skop and White, 1998). Dynactin might recruit dynein to these accumulation sites and the complex act to capture astral microtubules and exert a torque on the attached centrosomes, which rotationally aligns the spindle (Hyman, 1989; Hyman and White, 1987; Skop and White, 1998; Waddle et al., 1994). In order to identify whether dynactin is also involved in spindle alignment in extrinsically determined asymmetric divisions, we examined its role in EMS cell division. We found that dynactin is indeed required for EMS rotational spindle alignment and accumulates at the P2-EMS border prior to and during this process. The focal accumulation of dynactin depends on both Wnt and Src signaling. In addition, we present some evidence that indicates that the dynein-dynactin complex might be activated by the trimeric G-protein subunit Gα.

Results and Discussion

Generation of transgenic *dnc-1::gfp*, *dnc-2::gfp* and *arp-1::gfp* lines

In order to investigate the role of dynactin in EMS and P2 spindle alignment, *dynactin::gfp* transgenic lines were generated for the components *dnc-1*, *dnc-2* and *arp-1* (Le Bot et al., 2003; Skop and White, 1998). All the transgenic GFP lines were put under the *pie-1* promoter together with its 3′ UTR. To verify whether these GFP constructs were functional, expression of the native genes was suppressed by RNA interference (RNAi) targeted to the 3′ UTR sequences that were present only in the native genes. All of the three constructs tested in this way were functional, because 3′ UTR RNAi with the wild-type worms gave 100% dead embryos with no morphogenesis, whereas ~70-80% of the GFP embryos hatched as L1s with about half of the remaining embryos exhibiting partial morphogenesis. The reason that these GFP lines did not fully rescue the wild-type copies is probably because of the loss of transgenic protein expression when the *pie-1* promoter turns off in older embryos (Mello et al., 1996). We observed that the GFP localizations shifted from bright, diffuse cytoplasmic localization to more distinct structures in the DNC-2::GFP; *dnc-2 3′UTR RNAi* and ARP-1::GFP; *arp-1 3′UTR RNAi* embryos, whereas GFP localization in DNC-1::GFP; *dnc-1 3′UTR RNAi* embryos resembled DNC-1::GFP without RNAi (data not shown). These differing localizations are probably because the endogenous DNC-2 and ARP-1 were suppressed and therefore no longer competed with the transgene products for localization sites, allowing the GFPs to exhibit a more native localization. DNC-1::GFP was used in most analyses unless otherwise stated because its localization was not affected by the expression of the native *dnc-1* gene.

The dynactin complex becomes enriched at the P2-EMS border prior to and during EMS and P2 spindle rotation

When examined at the four-cell stage during P2 and EMS spindle rotation, DNC-1::GFP, DNC-2::GFP and ARP-1::GFP were all enriched at the cell border between P2 and EMS prior to and during EMS and P2 spindle rotation (Fig. 1A-C; supplementary material Movie 1). The accumulation first appeared at 8.88±0.63 minutes after the first appearance of the cleavage furrow in P1 (n=5, measured with DNC-2::GFP embryos) and remained there for 6.8±0.7 minutes (n=5). Dynactin-labeled EMS and P2 centrosomes rotated and moved such that one centrosome from each spindle became closely apposed to the accumulation site (Fig. 1A-C; supplementary material Movie 1). We also observed instances of dynactin-labeled putative microtubule (MT) plus-ends emanating from one centrosome and terminating at this accumulation site (Fig. 1A′; supplementary material Movie 1). The accumulation was then observed to disappear about 4.77±0.78 minutes (n=5) before EMS cleaved. This dynamic dynactin accumulation was

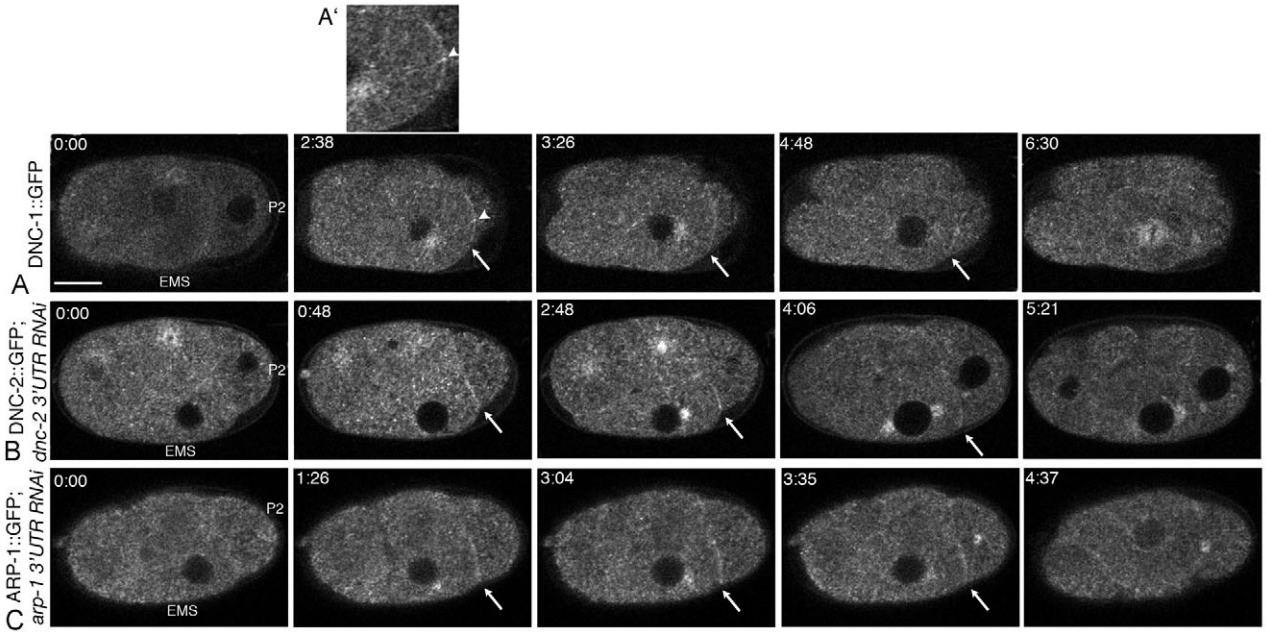

Fig. 1. Dynactin complex is enriched at the P2-EMS border prior to and during EMS and P2 spindle rotation. Multi-photon time series of embryos expressing (A) DNC-1::GFP (supplementary material Movie 1); (B) DNC-2::GFP; *dnc-2 3′UTR RNAi*; and (C) ARP-1::GFP; *arp-1 3′UTR RNAi* show the accumulation of dynactin along the P2-EMS border (marked by white arrows). 3′ UTR RNAi was used to improve the image contrast of DNC-2::GFP and ARP-1::GFP (see text). Notice that dynactin also localizes to centrosomes, serving as a marker for the spindle positioning. (A′) Enlarged region between the EMS centrosome and the P2-EMS accumulation in a DNC-1::GFP embryo. Arrowhead points to a dynactin-labeled astral MT plus-end that terminates at the accumulation site. Scale bar: 10 μm.

confirmed by immunofluorescence staining with anti-DNC-1 antibody (supplementary material Fig. S1A). Our observations are consistent with a model in which MT plus-ends are captured by sites of transiently accumulated dynactin. Dynactin along with dynein acts to pull the attached centrosome towards the cortex, thereby exerting a torque on the EMS and P2 spindles so as to rotationally align the spindles relative to the site of accumulation (Hyman, 1989; Hyman and White, 1987; Skop and White, 1998; Waddle et al., 1994).

Previous studies have shown that rotational alignment of the EMS spindle is different from that in P1: the former being a directed rotation, whereas the latter is a free rotation (Tsou et al., 2003). We also observed differences in that the enrichment of dynactin between P2 and EMS was a line instead of a defined spot as described for P0 and P1 (Skop and White, 1998; Waddle et al., 1994). How these different patterns of dynactin accumulation relate to the different spindle movements of P1 and EMS is not known, although it has been suggested that the broad accumulation might be responsible for cell-contact-dependent centrosome rotation, whereas the smaller one could be responsible for cell-autonomous centrosome rotation such as in P1 (Goldstein, 1995b).

Wnt and Src signaling are required for the asymmetric enrichment of dynactin at the P2-EMS border

We disrupted the Wnt pathway by knocking-down *mom-5* (encodes Fz receptor) by RNAi and found that, although EMS and P2 spindles still rotated (Bei et al., 2002; Thorpe et al., 1997), the dynactin::GFP enrichment was reduced (Fig. 2B,E; supplementary material Movie 2; *n*=10). Similarly, the dynactin::GFP enrichment was also reduced in the *src-1(RNAi)* (*C. elegans* Src) embryos (Fig. 2E; *n*=9), although, in this case, some alignment failures were observed (Bei et al., 2002; Walston et al., 2004). In cases in which the EMS spindle failed to rotate, dynactin accumulation was greatly reduced during EMS spindle positioning, although this accumulation increased prior to P2 spindle rotation (Fig. 2C; supplementary material Movie 2; *n*=3). When both spindles failed to rotate, dynactin accumulation remained at a low level throughout the cell cycle (Fig. 2C′; *n*=3).

Wnt and Src signaling have been shown to act together to control cleavage orientation in EMS (Bei et al., 2002; Walston et al., 2004). SRC-1 and MES-1 act in the Src pathway and signal bidirectionally between P2 and EMS to control division orientation in both EMS and P1 (Bei et al., 2002). When Wnt and Src signaling were disrupted simultaneously by *mom-5; src-1* double RNAi, we found that the dynactin::GFP enrichment at the P2-EMS border was eliminated throughout the entire P2-EMS cell cycle (Fig. 2D,E,G,G′; supplementary material Movie 4; *n*=10). At the same time, the EMS spindle orientation was completely inhibited, as reported (Bei et al., 2002; Walston et al., 2004), and we also observed failure of proper P2 spindle alignment in all the embryos examined (Fig. 2G,G′; supplementary material Movie 4; *n*=10). Similar dynactin localizations in different genetic backgrounds were also observed using anti-DNC-1-stained embryos (supplementary material Fig. S1B-D).

These observations indicate that Wnt and Src signaling act redundantly to regulate dynactin enrichment at P2-EMS borders, and that this localized accumulation is necessary for rotational alignment of both P1 and EMS spindles. It has been shown that the first 5 minutes into the EMS and P2 cell cycles is the critical time in which P2 can specify the future division axis of the EMS cell (Goldstein, 1995b). We found that dynactin::GFP accumulated at 8-9 minutes into the EMS and P2 cell cycles. We speculate that Wnt and Src signaling between P2 and EMS during the first 5 minutes are necessary to initiate the transportation of dynactin to the P2-EMS border. Our light-microscope observations cannot resolve whether the accumulated dynactin is in EMS, P2 or both cells. Future experiments with P2 and EMS blastomere isolation and re-assembly might shed light on this issue. However, our observation that rotational alignment fails in both P2 and EMS suggests that the accumulation is occurring in both. It remains to be determined how the Wnt pathway signals back from EMS to P2 to direct P2 spindle orientation and what the downstream targets are that transport dynactin to the P2-EMS border.

Dynactin::GFP enrichment at the P2-EMS border is not fully abolished in Gα mutant embryos

Gα, one of the trimeric G-protein subunits, is required for the rotational alignment of the P0 and EMS spindles (Tsou et al., 2003). There are two redundant Gα proteins, GOA-1 and GPA-16 (Gotta and Ahringer, 2001). We explored whether Gα regulates dynactin::GFP localization or its activation at the P2-EMS border. In order to knock-down both Gα proteins during EMS and P2 divisions without affecting early cell divisions, we used partial *goa-1* RNAi treatment in *gpa-16(it143ts)*; *dnc-1::gfp* embryos at permissive temperature, and then shifted the embryos to the restrictive temperature at the four-cell stage. We found that not only were the spindle alignments in the anterior daughter cell (ABa) and the posterior daughter cell (ABp) perturbed as reported (Bergmann et al., 2003), but both EMS and P2 spindles failed to rotate to the A-P axis (Fig. 2H; *n*=9), yet dynactin localization at the P2-EMS contact site was still retained. One caveat of this experiment was that DNC-1::GFP gave a strong cytoplasmic signal when grown at permissive temperature, making it difficult to see the cortical accumulation of dynactin::GFP. Nevertheless, we clearly observed weak dynactin::GFP enrichment at P2-EMS border in Gα mutant embryos (Fig. 2H; supplementary material Movie 5; *n*=3). This weak accumulation was comparable with the wild-type control, although it was at the lower end of the wild-type intensity range (Fig. 2I).

Depleting Gα did not totally abolish dynactin localization at the P2-EMS border; nevertheless, rotational alignment in P2 and EMS spindles was completely inhibited. It might be that the residual dynactin was insufficient to mediate the rotational alignment of the P2 and EMS spindles. However, we suspect that Gα might be involved in directly regulating the activity of dynactin, because the P2-EMS border enrichment of GPR-1/2, the activator of Gα, is dependent on the Src but not the Wnt pathway (Tsou et al., 2003). If Gα/GPR-1/2 was responsible for dynactin::GFP enrichment at the P2-EMS border, one would not therefore expect dynactin accumulation to be affected when Wnt signaling was disrupted. By contrast, our observations show that dynactin::GFP enrichment at the P2-EMS border depends on both Wnt and Src.

Dynactin activity is required for EMS spindle rotation

Our observations suggest that dynactin::GFP is localized at the right place and right time to mediate P2 and EMS spindle rotations. However, direct examination of the role of dynactin in EMS and P2 spindle orientation is difficult because dynactin is also required for many aspects of early divisions (Gonczy et al., 1999a; Skop and White, 1998). Temperature-sensitive mutants provide a way of removing a gene product at a specific time. A weak *dnc-1(or404ts)* mutant has been isolated (Encalada et al., 2005). For the P0 cell,

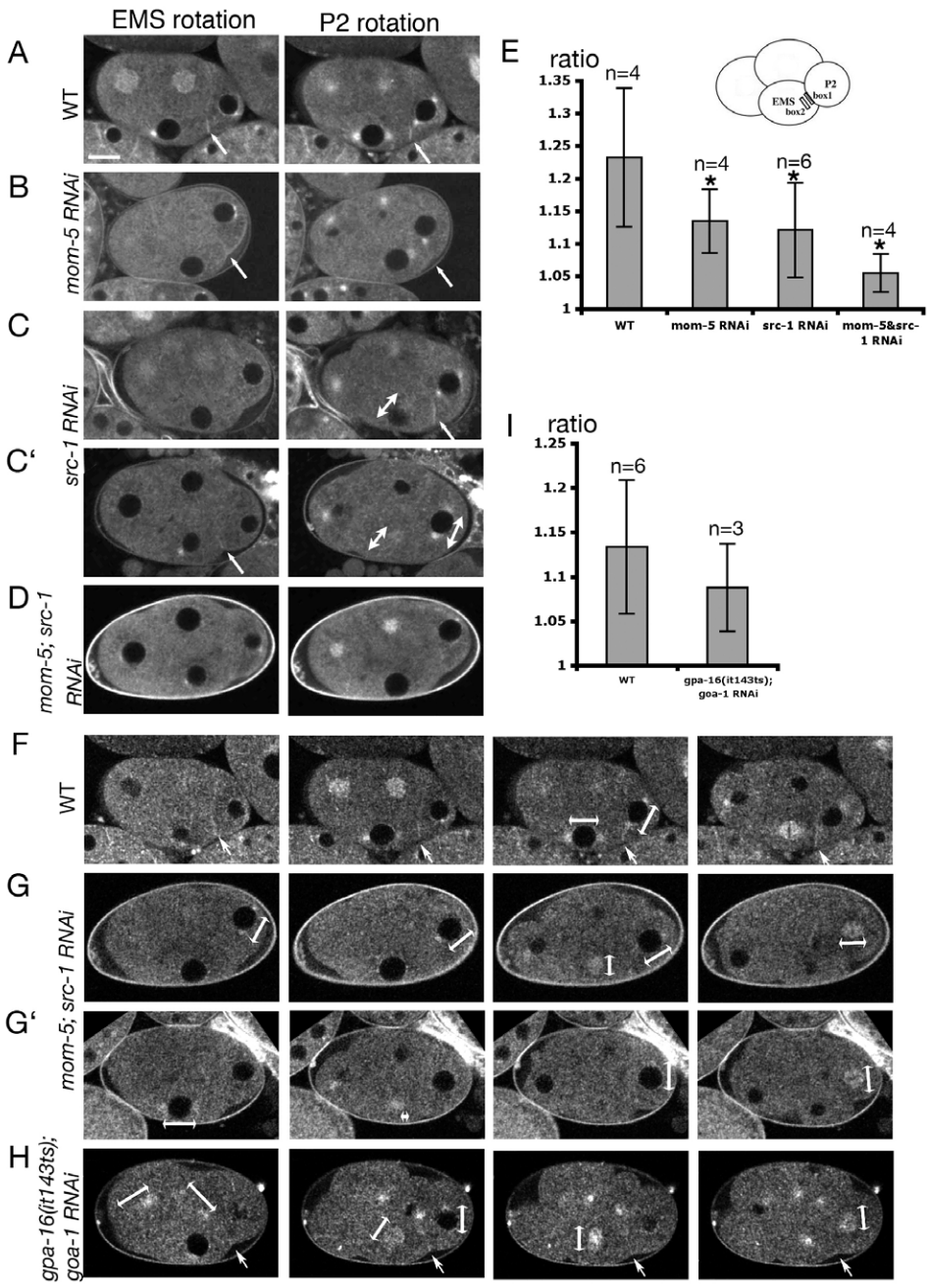

Fig. 2. Dynactin::GFP enrichment at the P2-EMS border is regulated by both the Wnt and Src pathways, but not by Gα. P2 cell is to the right and EMS is at the bottom. Dynactin accumulation to the P2-EMS border is dynamic. In order to compare the fluorescence intensity among varied genetic backgrounds over a period of time, we selected ten adjacent frames (total 44 seconds) and projected these in ImageJ to produce an averaged image of this time interval. Intervals were chosen to show the best accumulation in (A) DNC-1::GFP wild type (WT); (B) DNC-1::GFP with *mom-5* RNAi (supplementary material Movie 2); (C,C′) DNC-1::GFP with *src-1* RNAi (supplementary material Movie 3); and (D) DNC-1::GFP with *mom-5; src-1* RNAi. In C, the spindle of P2 but not EMS rotates, whereas, in C′, neither the P2 nor EMS spindle rotates. Arrows mark P2-EMS dynactin accumulation. Double-headed arrows show the misaligned spindles in *src-1 RNAi* embryos. (E) Quantitative analysis of the fluorescence intensity along the P2-EMS border using ImageJ. Two 25×7 pixel boxes were drawn in each of the generated averaged images, one along the P2-EMS border (box 1) and the other in the cytoplasm below this accumulation (box 2). A ratio of box1:box 2 fluorescence intensity is plotted for different genetic backgrounds. Error bars are s.d. Asterisks indicate a statistically significant difference ($P<0.05$) between wild-type and the RNAi-treated embryos (Student's *t*-test, two-tailed equal variance). (F-H) Multi-photon time series of embryos expressing DNC-1::GFP show the P2-EMS accumulation (white arrows), and P2 and EMS spindle positioning (double-headed arrows). In a wild-type embryo (F), DNC-1 accumulates at the P2-EMS border prior to and during EMS and P2 spindle rotations. The two spindles rotate and move such that one centrosome from each is adjacent to this accumulation site. In a *mom-5; src-1 RNAi* embryo (G), P2 centrosomes rotate partially but the final position of the spindle is away from the P2-EMS border ($n=7$); whereas, in another *mom-5; src-1 RNAi* embryo (G′; supplementary material Movie 4), P2 centrosomes fail to rotate and spindle forms along the D-V axis ($n=3$). In both cases, EMS spindle fails to align along the A-P axis, and DNC-1::GFP does not accumulate at the P2-EMS border. (H; supplementary material Movie 5) In *gpa-16(it143ts);goa-1(RNAi)* embryos, DNC-1::GFP still accumulates at the P2-EMS border, albeit weakly (see text). All the spindle orientations, including ABa, ABp, EMS and P2, are abnormal. (I) Quantitative analysis of the fluorescence intensity along the P2-EMS border between wild-type DNC-1::GFP and *gpa-16(it143ts);goa-1(RNAi)* embryos grown at permissive temperature. Measurements were taken as in E. There is no statistically significant difference ($P=0.20$) between wild-type and the Gα mutant embryos (Student's *t*-test, two-tailed equal variance). Scale bar: 10 μm.

shifting the *dnc-1(or404ts)* embryos to the restrictive temperature just before centrosome centration led to P0 spindle rotation failure (supplementary material Fig. S2B). In order to perturb the P1 spindle rotation, the *dnc-1(or404ts)* embryos needed to be shifted to the restrictive temperature during one-cell metaphase (supplementary material Fig. S2D). However, shifting the embryos during P1 division did not lead to EMS and P2 spindle rotation defect (data not shown). This indicates that the activity of the mutant DNC-1 protein was still sufficient to promote the rotation of the EMS and P2 spindles when the cell sizes were reduced.

To make the weak *dnc-1(ts)* allele more sensitive to temperature shifts, we used a partial RNAi treatment to deplete just enough of the mutated DNC-1 protein, so that the remaining level was still sufficient to allow normal early divisions at the permissive temperature. We then shifted the embryos to the restrictive temperature during the P1 cell cycle (just prior to or after P1 spindle rotation) to observe the EMS and P2 divisions. By increasing the hours of RNAi treatment, the *dnc-1(or404ts)* embryos initially divided normally, then the EMS spindle failed to rotate, and finally the RNAi effect was too strong and the early divisions were affected (Fig. 3C; data not shown). In wild-type embryos, the two EMS centrosomes are first aligned along the L-R axis, then they rotate onto the A-P axis before the nuclear envelope breakdown (Hyman and White, 1987) (Fig. 3A). In *dnc-1(or404ts);dnc-1 RNAi* embryos, while subjected to the restrictive temperature, the EMS centrosomes failed to rotate to the A-P axis. Consequently, the metaphase EMS spindle set up along either the L-R axis (Fig. 3C; perpendicular to the A-P axis; n=3) or the D-V axis (n=5). In the D-V configuration, one of the centrosomes was out of focus so the angle of the spindle to the A-P axis could not be determined. However, the geometry of the metaphase spindle was such that the spindle had to be orientated to within about ±45° of the D-V axis for only one centrosome to be visible. During anaphase, the transverse EMS spindle elongated and then flipped onto the A-P axis, probably due to constraints of the egg shell. We did not detect a complete failure of P2 spindle rotation in this experimental situation before the RNAi disrupted the early divisions. Given that dynactin is required for spindle rotation in other P-lineage cells (P0 and P1) (Gonczy et al., 1999a; Skop and White, 1998) (supplementary material Fig. S2B,D), we suggest that it is likely that dynactin might be involved in P2 spindle rotation as well. Our failure to detect P2 misalignments with the weak *dnc-1(or404ts)* allele indicates that P2 spindle rotation requires even less dynactin activity than EMS. Owing to the involvement of dynactin in many aspects of cell division, the effect on gut cell fate due to a misaligned EMS spindle was not determined.

In summary, we found that both Wnt and Src signaling contribute to dynactin accumulation to the P2-EMS border. Although Gα might not be required for dynactin::GFP enrichment, we suggest that it might regulate the motor activity of dynactin. Gα/GPR-1/2 is regulated differently by Wnt and Src, in that GPR-1/2 is enriched at the P2-EMS border in response to the Src but not the Wnt pathway (Tsou et al., 2003). LET-99 inhibits GPR-1/2 enrichment at the P2-EMS border (Tsou et al., 2003); however, the role of LET-99 in dynactin enrichment has not been determined. Based on the above results, we propose a model for the role of dynactin in transducing polarizing signals during nuclear rotation in P2 and EMS cells (Fig. 4). Wnt- and Src-mediated dynactin accumulation at the P2-EMS border serves as a focal MT capture site to bring about the Gα-regulated rotational alignment of the EMS and/or P2 spindles, a function that could well be conserved in other organisms (Busson et al., 1998; Dujardin and Vallee, 2002; Lechler and Fuchs, 2005; Schuyler and Pellman, 2001).

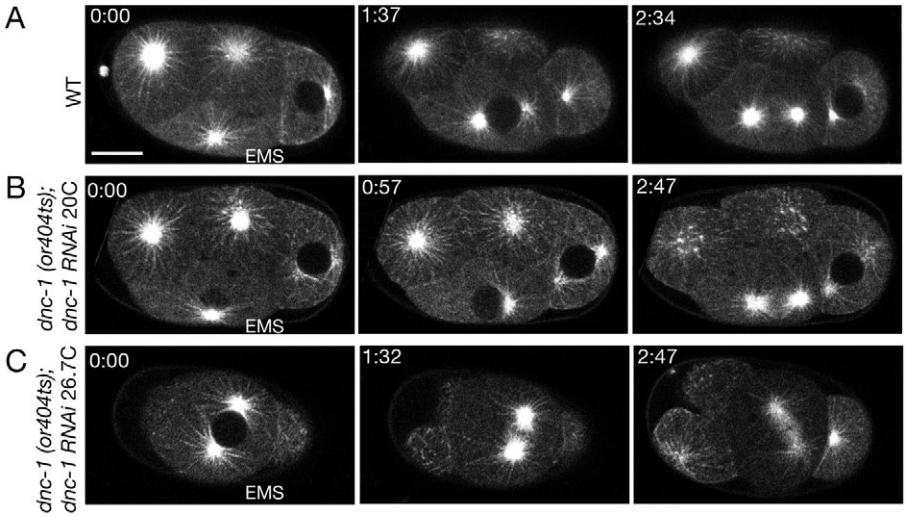

Fig. 3. Dynactin activity is required at least for EMS spindle rotation. Multi-photon time series of embryos expressing tubulin::GFP in (A) wild type (WT) and (B) *dnc-1(or404ts)* embryos treated with partial *dnc-1* RNAi (see Materials and Methods) and imaged at permissive temperature showed normal EMS spindle rotation; (C) *dnc-1(or404ts)* embryos treated with partial *dnc-1* RNAi and imaged at restrictive temperature showed EMS set up its metaphase spindle perpendicular to the A-P axis (this embryo shows a ventral aspect). Scale bar: 10 μm.

Materials and Methods

C. elegans strains

All worm strains were maintained as described (Brenner, 1974). The following strains were used: N2, wild type; WH257, *unc-119(ed3); ojIs5[dnc-1::gfp unc-119(+)]*; WH258, *unc-119(ed3); ojIs57[dnc-2::gfp unc-119(+)]*; WH259, *unc-119(ed3); ojIs47[arp-1::gfp unc-119(+)]*; BW1809, *gpa-16(it143) I; him-5(e1490) V* (Bergmann et al., 2003); WH456, *gpa-16(it143) I; him-5(e1490) V; ojIs5[dnc-1::gfp unc-119(+)]*; WH204, *unc-119(ed3); ojIs1[beta-tubulin::gfp unc-119(+)]* (Strome et al., 2001); EU1006, *dnc-1(or404) IV* (Encalada et al., 2005); WH441, *dnc-1(or404) IV; ojIs1[beta-tubulin::gfp unc-119(+)]*; EU311, *dpy-5(e61) mom-5(or57)/hT2 I; +/hT2[bli-4(e937) let-?(h661)] III* (Thorpe et al., 1997); and SS149, *mes-1(bn7)X* (Capowski et al., 1991).

We grew EU311worms at 20°C and used the dumpy worms that were homozygous for the mutation for analysis. SS149 was maintained at 16°C and shifted to 25°C

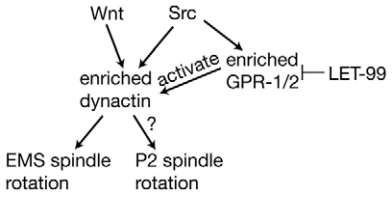

Fig. 4. Model for the role of dynactin in receiving polarized signals during nuclear rotation in P2 and EMS (see text).

overnight before analysis. WH441 and WH456 were also maintained at 16°C and shifted to its restrictive temperature (26.7°C for WH441 and 25°C for WH456) just before analysis.

RNAi treatment

RNAi against the dynactin 3′ UTR was carried out as described (McMahon et al., 2001). The following primers (shown 5′ to 3′) were used to amplify the 3′ UTR sequence from either cDNAs (*dnc-1*, yk11c8; *dnc-2*, yk569h8 and *arp-1*, yk455a10) or genomic DNAs (T7 site in bold). *dnc-1* forward, **TAATACGACTCACTATA**CGTGTGGTAGACTGCCGAAATTC, reverse, **TAATACGACTCACTATA**AACGCACCTCAAAACAGTGC; *dnc-2* forward, **TAATACGACTCACTATAG**TGGCAGATTTGAAGTG, reverse, **TAATACGACTCACTATA**CTGAATAGAGATTGGTTCATTCGG; *arp-1* forward, **TAATACGACTCACTATA**TTTCCCCCTTTTTCTCCC, reverse, **TAATACGACTCACTATA**GAAACAGGCATAAAGCAG.

dsRNAs were then produced using the in vitro T7 MEGAshortscript High Yield Transcription Kit (Ambion). 3~5 mg/ml dsRNAs were used either to soak N2 L4 larvae or to inject into N2 young adults and analyzed 40 hours later (Fire et al., 1998; Tabara et al., 1998). For *mom-5* and *src-1* RNAi by injection, dsRNAs (3 mg/ml each) were synthesized using T3 and T7 in vitro transcription kits (Ambion) with cDNA clones yk417a5 and yk117f2. For *mom-5; src-1* double RNAi, RNAs from each gene were mixed up (1.5 mg/ml each) for injection. Embryos were analyzed 40 hours after injection. *goa-1* RNAi feeding vector was obtained from Ahringer's feeding library (Kamath et al., 2003). The *dnc-1* feeding vector was constructed by cloning the full-length cDNA yk11c8 into the feeding vector L4440 and then transformed into HT115 bacteria (Timmons and Fire, 1998). RNAi feeding experiments were performed as described (Fire et al., 1998; Timmons and Fire, 1998).

Live imaging

Slides for live imaging were prepared by either mounting on a 3% agar pad or in a hanging drop in Egg Buffer. Four-dimensional Nomarski imaging was performed as described previously (Skop and White, 1998). We used a Nikon Optiphot-2 upright microscope with a Nikon PlanApo 60× 1.4 NA DIC lens and a Hamamatsu C2400 CCD camera or a Nikon Diaphot300 inverted microscope with a 60× 1.4 NA DIC lens and a Sony XC-75 CCD camera. All GFP imaging was performed by multi-photon excitation with an optical workstation (OWS) (Nazir, M. Z., Eliceiri, K., Ahmed, A., Agarwal, V., Rao, Y., Kumar, S., Lukas, T., Nasim, M., Hashmi, A., Rueden, C. et al., submitted), which consists of a Nikon Eclipse TE300DV inverted microscope with either a Nikon Super Fluor 100× 1.3 NA lens or a PlanApo VC 60× 1.4 NA. The excitation source was a Ti:sapphire laser tuned to 890 nm. The detector was a high quantum efficiency Hamamatsu H7422-40 detector (Hamamatsu Photonics, Hamamatsu City, Japan). Images were collected at 512×512 pixel resolution at 4.5-second intervals and analyzed with ImageJ v. 1.37 (http://rsb.info.nih.gov/ij/). The dynactin::GFP movies for which frames are shown in Fig. 2 were smoothed with ImageJ to reduce background noise.

Dynactin::GFP

Full-length *dnc-1* and *dnc-2* were amplified from genomic DNA, whereas full-length *arp-1* was amplified from cDNA yk455a10. All three genes were cloned into the plasmid pFJ1.1 (Squirrell et al., 2006). The plasmids were then bombarded into *unc-119* worms as described (Praitis et al., 2001). Worms were allowed to grow for at least 2 weeks. The rescued worms were examined for GFP expression.

Antibody production and immunohistochemistry

The following peptide sequence Ac-DPNEPQFTAPDPRRQSLC-amide was used to generate rabbit polyclonal anti-DNC-1 antibody. Protein production, antibody production and affinity purification were performed by Quality Controlled Biochemicals (Hopkinton, MA). Western blot with anti-DNC-1 antibody was carried out as described (Squirrell et al., 2006), using 1:3000 dilution. Antibody staining was performed as described (Gonczy et al., 1999b). Slides were viewed on a Bio-Rad MRC1024 confocal microscope (Hercules, CA). Images were prepared for publication with Adobe Photoshop (version 8.0). Antibodies were diluted as follows: DM1α, mouse anti-α-tubulin, 1:200 (Sigma, St Louis, MO); rabbit anti-DNC-1, 1:400. DNA was labeled using DAPI (1.5 μg/ml).

dnc-1 RNAi in *dnc-1(or404ts)* worms

In order to titrate down the DNC-1 function in *dnc-1(or404ts)* worms for the quick-temperature-shifting experiment, *dnc-1(or404)* worms were fed on a diluted *dnc-1* RNAi plate (diluted to 1/7 with HT115) at 16°C for 20-21 hours, or on a normal *dnc-1* RNAi plate at 19°C for 5-6 hours. Embryos at P1 division were then shifted to 26.7°C and imaged on OWS for observing EMS and P2 spindle rotation defects.

goa-1 RNAi in *gpa-16 (it143ts)* worms

In order to knock-down both *goa-1* and *gpa-16* during EMS and P2 divisions without affecting early cell divisions, *gpa-16(it143ts)*; *dnc-1::gfp* worms were fed on *goa-1* RNAi plates at 16°C for 26 hours or 20°C for 4 hours. The embryos were then shifted to 25°C at the four-cell stage to image on the OWS.

We would like to thank Yuji Kohara and CGC for reagents. This work was supported by a grant from the National Institutes of Health to J.G.W. (GM052454-09).

References

Ahringer, J. (2003). Control of cell polarity and mitotic spindle positioning in animal cells. *Curr. Opin. Cell Biol.* **15**, 73-81.

Bei, Y., Hogan, J., Berkowitz, L. A., Soto, M., Rocheleau, C. E., Pang, K. M., Collins, J. and Mello, C. C. (2002). SRC-1 and Wnt signaling act together to specify endoderm and to control cleavage orientation in early C. elegans embryos. *Dev. Cell* **3**, 113-125.

Bergmann, D. C., Lee, M., Robertson, B., Tsou, M. F., Rose, L. S. and Wood, W. B. (2003). Embryonic handedness choice in C. elegans involves the Galpha protein GPA-16. *Development* **130**, 5731-5740.

Bowerman, B., Ingram, M. K. and Hunter, C. P. (1997). The maternal par genes and the segregation of cell fate specification activities in early Caenorhabditis elegans embryos. *Development* **124**, 3815-3826.

Brenner, S. (1974). The genetics of Caenorhabditis elegans. *Genetics* **77**, 71-94.

Busson, S., Dujardin, D., Moreau, A., Dompierre, J. and De Mey, J. R. (1998). Dynein and dynactin are localized to astral microtubules and at cortical sites in mitotic epithelial cells. *Curr. Biol.* **8**, 541-544.

Capowski, E. E., Martin, P., Garvin, C. and Strome, S. (1991). Identification of grandchildless loci whose products are required for normal germ-line development in the nematode Caenorhabditis elegans. *Genetics* **129**, 1061-1072.

Dujardin, D. L. and Vallee, R. B. (2002). Dynein at the cortex. *Curr. Opin. Cell Biol.* **14**, 44-49.

Encalada, S. E., Willis, J., Lyczak, R. and Bowerman, B. (2005). A spindle checkpoint functions during mitosis in the early Caenorhabditis elegans embryo. *Mol. Biol. Cell* **16**, 1056-1070.

Fire, A., Xu, S., Montgomery, M. K., Kostas, S. A., Driver, S. E. and Mello, C. C. (1998). Potent and specific genetic interference by double-stranded RNA in Caenorhabditis elegans. *Nature* **391**, 806-811.

Goldstein, B. (1992). Induction of gut in Caenorhabditis elegans embryos. *Nature* **357**, 255-257.

Goldstein, B. (1993). Establishment of gut fate in the E lineage of C. elegans: the roles of lineage-dependent mechanisms and cell interactions. *Development* **118**, 1267-1277.

Goldstein, B. (1995a). An analysis of the response to gut induction in the C. elegans embryo. *Development* **121**, 1227-1236.

Goldstein, B. (1995b). Cell contacts orient some cell division axes in the Caenorhabditis elegans embryo. *J. Cell Biol.* **129**, 1071-1080.

Goldstein, B. (2000). When cells tell their neighbors which direction to divide. *Dev. Dyn.* **218**, 23-29.

Gonczy, P., Pichler, S., Kirkham, M. and Hyman, A. A. (1999a). Cytoplasmic dynein is required for distinct aspects of MTOC positioning, including centrosome separation, in the one cell stage Caenorhabditis elegans embryo. *J. Cell Biol.* **147**, 135-150.

Gonczy, P., Schnabel, H., Kaletta, T., Amores, A. D., Hyman, T. and Schnabel, R. (1999b). Dissection of cell division processes in the one cell stage Caenorhabditis elegans embryo by mutational analysis. *J. Cell Biol.* **144**, 927-946.

Gotta, M. and Ahringer, J. (2001). Distinct roles for Galpha and Gbetagamma in regulating spindle position and orientation in Caenorhabditis elegans embryos. *Nat. Cell Biol.* **3**, 297-300.

Guo, S. and Kemphues, K. J. (1996). Molecular genetics of asymmetric cleavage in the early Caenorhabditis elegans embryo. *Curr. Opin. Genet. Dev.* **6**, 408-415.

Horvitz, H. R. and Herskowitz, I. (1992). Mechanisms of asymmetric cell division: two Bs or not two Bs, that is the question. *Cell* **68**, 237-255.

Hyman, A. A. (1989). Centrosome movement in the early divisions of Caenorhabditis elegans: a cortical site determining centrosome position. *J. Cell Biol.* **109**, 1185-1193.

Hyman, A. A. and White, J. G. (1987). Determination of cell division axes in the early embryogenesis of Caenorhabditis elegans. *J. Cell Biol.* **105**, 2123-2135.

Kamath, R. S., Fraser, A. G., Dong, Y., Poulin, G., Durbin, R., Gotta, M., Kanapin, A., Le Bot, N., Moreno, S., Sohrmann, M. et al. (2003). Systematic functional analysis of the Caenorhabditis elegans genome using RNAi. *Nature* **421**, 231-237.

Le Bot, N., Tsai, M. C., Andrews, R. K. and Ahringer, J. (2003). TAC-1, a regulator of microtubule length in the C. elegans embryo. *Curr. Biol.* **13**, 1499-1505.

Lechler, T. and Fuchs, E. (2005). Asymmetric cell divisions promote stratification and differentiation of mammalian skin. *Nature* **437**, 275-280.

McMahon, L., Legouis, R., Vonesch, J. L. and Labouesse, M. (2001). Assembly of C. elegans apical junctions involves positioning and compaction by LET-413 and protein aggregation by the MAGUK protein DLG-1. *J. Cell Sci.* **114**, 2265-2277.

Mello, C. C., Schubert, C., Draper, B., Zhang, W., Lobel, R. and Priess, J. R. (1996). The PIE-1 protein and germline specification in C. elegans embryos. *Nature* **382**, 710-712.

Praitis, V., Casey, E., Collar, D. and Austin, J. (2001). Creation of low-copy integrated transgenic lines in Caenorhabditis elegans. *Genetics* **157**, 1217-1226.

Roegiers, F. and Jan, Y. N. (2004). Asymmetric cell division. *Curr. Opin. Cell Biol.* **16**, 195-205.

Schlesinger, A., Shelton, C. A., Maloof, J. N., Meneghini, M. and Bowerman, B. (1999). Wnt pathway components orient a mitotic spindle in the early Caenorhabditis elegans embryo without requiring gene transcription in the responding cell. *Genes Dev.* **13**, 2028-2038.

Schroer, T. A. (2004). Dynactin. *Annu. Rev. Cell Dev. Biol.* **20**, 759-779.

Schuyler, S. C. and Pellman, D. (2001). Search, capture and signal: games microtubules and centrosomes play. *J. Cell Sci.* **114**, 247-255.

Skop, A. R. and White, J. G. (1998). The dynactin complex is required for cleavage plane specification in early Caenorhabditis elegans embryos. *Curr. Biol.* **8**, 1110-1116.

Squirrell, J. M., Eggers, Z. T., Luedke, N., Saari, B., Grimson, A., Lyons, G. E., Anderson, P. and White, J. G. (2006). CAR-1, a protein that localizes with the mRNA decapping component DCAP-1, is required for cytokinesis and ER organization in Caenorhabditis elegans embryos. *Mol. Biol. Cell* **17**, 336-344.

Strome, S., Powers, J., Dunn, M., Reese, K., Malone, C. J., White, J., Seydoux, G. and Saxton, W. (2001). Spindle dynamics and the role of gamma-tubulin in early Caenorhabditis elegans embryos. *Mol. Biol. Cell* **12**, 1751-1764.

Tabara, H., Grishok, A. and Mello, C. C. (1998). RNAi in C. elegans: soaking in the genome sequence. *Science* **282**, 430-431.

Thorpe, C. J., Schlesinger, A., Carter, J. C. and Bowerman, B. (1997). Wnt signaling polarizes an early C. elegans blastomere to distinguish endoderm from mesoderm. *Cell* **90**, 695-705.

Timmons, L. and Fire, A. (1998). Specific interference by ingested dsRNA. *Nature* **395**, 854.

Tsou, M. F., Hayashi, A. and Rose, L. S. (2003). LET-99 opposes Galpha/GPR signaling to generate asymmetry for spindle positioning in response to PAR and MES-1/SRC-1 signaling. *Development* **130**, 5717-5730.

Waddle, J. A., Cooper, J. A. and Waterston, R. H. (1994). Transient localized accumulation of actin in Caenorhabditis elegans blastomeres with oriented asymmetric divisions. *Development* **120**, 2317-2328.

Walston, T., Tuskey, C., Edgar, L., Hawkins, N., Ellis, G., Bowerman, B., Wood, W. and Hardin, J. (2004). Multiple Wnt signaling pathways converge to orient the mitotic spindle in early C. elegans embryos. *Dev. Cell* **7**, 831-841.